Anal. Chem. **1998,** *70,* 4701−4708

Simultaneous Multispectral Imaging in the Visible and Near-Infrared Region: Applications in Document Authentication and Determination of Chemical Inhomogeneity of Copolymers

Chieu D. Tran,* Yan Cui, and Sergey Smirnov

Department of Chemistry, Marquette University P.O. Box 1881, Milwaukee, Wisconsin 53201

A new multispectral imaging spectrometer capable of simultaneously recording spectral images in the visible and near-infrared has been developed. In this instrument, an acoustooptic tunable filter is used to diffract an unpolarized incident light into two diffracted beams with orthogonal polarization; one of them is detected by a silicon camera for the visible region while the other beam is detected in the near-infrared region (from 1 to 1.7 μm) with a NIR camera. The imaging spectrometer is sensitive, inexpensive, and field deployable because it is based on the recently available InGaAs focal plane arrays camera, which is low cost and can be sensitively operated at room temperature. Preliminary applications of the imaging spectrometer include measurements of the visible and NIR absorption spectra of ink used to print U.S. currency. Such results may help to characterize samples as well as to control and to ensure the quality of the samples during the production processes. More important are the results obtained on ethylene/vinyl acetate copolymers. The NIR spectral images obtained clearly indicate that these copolymers exhibit a high degree of chemical inhomogeneity. Because of the possibility of inhomogeneity, it is very important that the homogeneity of polymers or copolymers be thoroughly understood before the NIR methods, especially those based on NIR spectrometers equipped with a single-element detector, are used for measurements.

A multispectral imaging spectrometer is an instrument that can simultaneously record spectral and spatial information of a sample; i.e., the recorded images contain signals that are generated by molecules or units in a sample, plotted as a function of spectral and spatial distribution.[1] Chemical homogeneity of the sample can be elucidated from such images. This type of information is of particular importance since it is known that chemical as well as physical properties of materials are dependent on the chemical distribution within the samples. As a consequence, considerable efforts have been made in the past few years to develop multispectral imaging instruments. In these instruments, the spatial distribution of the sample is obtained by a camera, and the spectral information is gained by scanning a dispersive element to record spectra for each image.[1] Mechanical scanning dispersive devices (filter wheels, monochromators) are not desirable because they are slow and prone to vibrations. Spectral tunable filters based on electronic tuning such as an acoustooptic tunable filter, are desirable as they are fast and compact and have no moving parts.

An acoustooptic tunable filter (AOTF) is a solid-state electronically tunable spectral band-pass filter which is based on the diffraction of light by an acoustic wave in an anisotropic crystal.[2−10] Compared to other dispersive devices, the AOTF offers such advantages as being all solid state, having rapid scanning ability (μs), high diffraction efficiency, and wide spectral tuning range, giving high resolution (2−6 Å), and offering imaging capability.[2−10] The filter is, therefore, particularly suited for multispectral imaging instruments.

Multispectral imaging instruments based on AOTF have, in fact, been developed. In these instruments, the tunable filter was used to disperse light in either the visible or the near-infrared (NIR) region, and the corresponding spatial information was then obtained with either a silicon CCD camera or an indium antimonide (InSb) camera.[11−18] As such, these instruments have not exploited the full potentials of the AOTF. Specifically, in these instruments, only one of two diffracted light beams from the AOTF was used. As a consequence, multispectral imaging can only be

(1) Morris, M. D. *Microscopic and Spectroscopic Imaging of the Chemical State*; Marcel Dekker: New York, 1993.
(2) Tran, C. D. *Anal. Chem.* **1992**, *64*, 971A−981A.
(3) Tran, C. D.; Bartelt, M. *Rev. Sci. Instrum.* **1992**, *63*, 2939.
(4) Tran, C. D.; Furlan, R. J. *Anal. Chem.* **1992**, *64*, 2775−2782.
(5) Tran, C. D.; Furlan, R. J. *Anal. Chem.* **1993**, *65*, 1675−1681.
(6) Tran, C. D.; Lu, J. *Anal. Chim. Acta* **1995**, *314*, 57−66.
(7) Baptista, M. S.; Tran, C. D.; Gao, G. H. *Anal. Chem.* **1996**, *68*, 971−976.
(8) Tran, C. D. *Talanta* **1997**, *45*, 237−248.
(9) Baptista, M. S.; Tran, C. D. *Appl. Opt.* **1997**, *36*, 7059−7065.
(10) Alexander, T. A.; Gao, G. H.; Tran, C. D. *Appl. Spectrosc.* **1997**, *51*, 1603−1606.
(11) Treado, P. J.; Levin, I. W.; Lewis, E. N. *Appl. Spectrosc.* **1992**, *46*, 553−559.
(12) Treado, P. J.; Levin, I. W.; Lewis, E. N. *Appl. Spectrosc.* **1992**, *46*, 1211−1216.
(13) Treado, P. J.; Levin, I. W.; Lewis, E. N. *Appl. Spectrosc.* **1994**, *48*, 607−615.
(14) Morris, H. R.; Hoyt, C. C.; Treado, P. J. *Appl. Spectrosc.* **1994**, *48*, 857−866.
(15) Pallister, D. M.; Govil, A.; Morris, M. D.; Colburn, W. S. *Appl. Spectrosc.* **1994**, *48*, 1015−1020.
(16) Schaeberle, M. D.; Karakatsanis, C. G.; Lau, C. J.; Treado, P. *J. Anal. Chem.* **1995**, *67*, 4316−4321.
(17) Schaeberle, M. D.; Kalasinsky, V. F.; Luke, J. L.; Lewis, E. N.; Levin, I. W.; Treado, P. J. *Anal. Chem.* **1996**, *68*, 1829−1833.
(18) Schaeberle, M. D.; Karakatsanis, C. G.; Lau, C. J.; Treado, P. J. *Anal. Chem.* **1995**, *67*, 4318−4321.

10.1021/ac980647q CCC: $15.00
Published on Web 10/09/1998

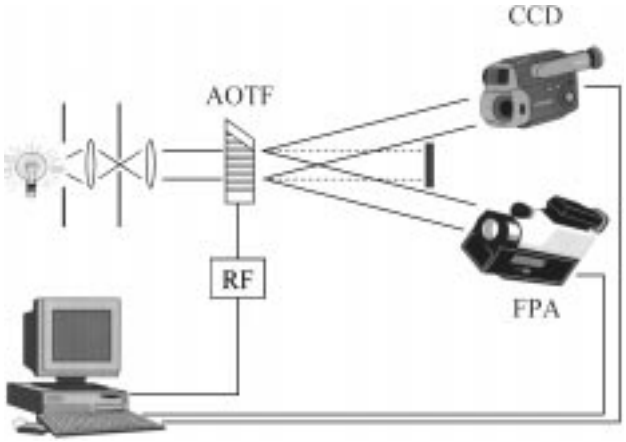

Figure 1. Schematic diagram of the imaging spectrometer: AOTF, acoustooptic tunable filter; RF, rf signal generator, CCD, charge-coupled device camera for the visible; FPA, InGaAs focal plane array camera for the near-infrared region.

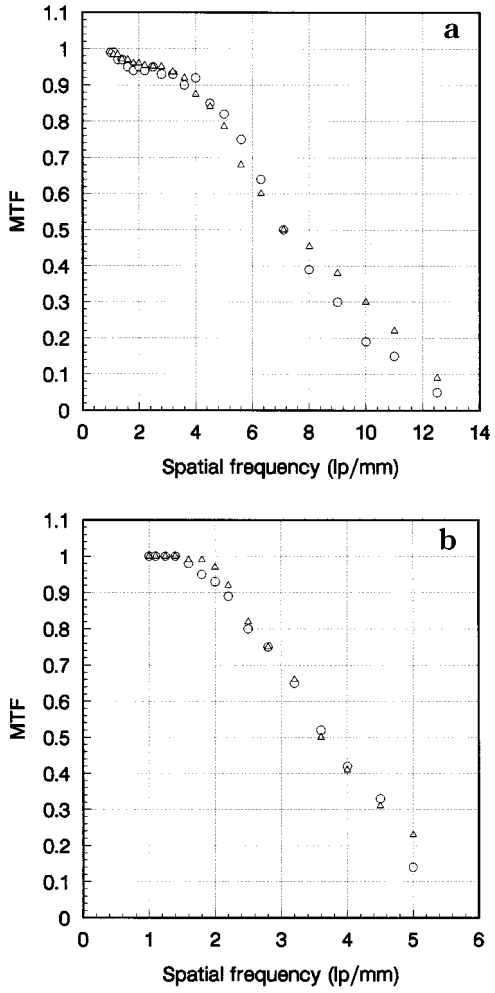

Figure 2. Modulation transfer function (MTF) as a function of spatial frequency measured at (a) 650 nm with the CCD camera and at 1400 nm (b) with the InGaAs camera: (○) with ADTF and (△) with interference filter.

obtained in either the visible or the NIR region but not both. This is rather unfortunate because it is possible to use the AOTF to simultaneously record spectral and spatial information in both regions. This possibility stems from the fact that the AOTF has

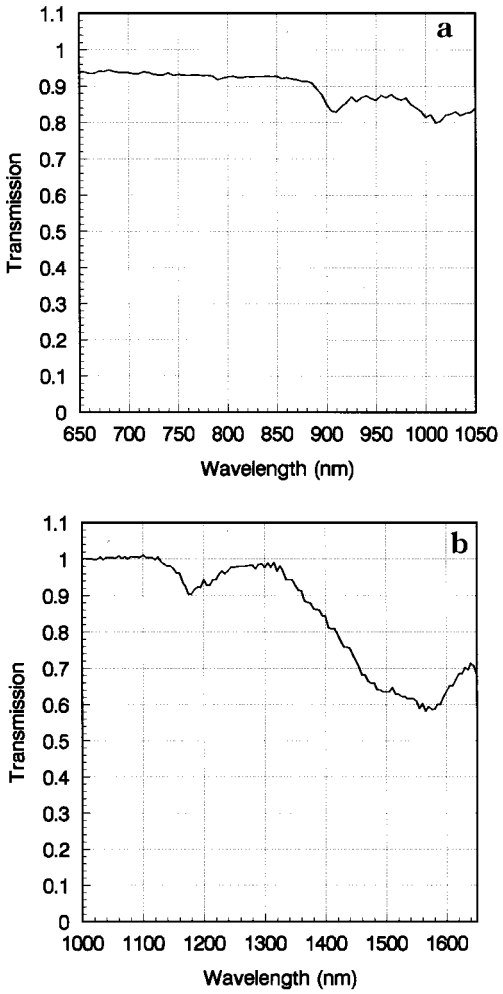

Figure 3. Transmission spectrum of ethanol in 1-cm cell measured with the CCD (a) and with the InGaAs (b) camera.

much wider spectral tuning range than conventional grating monochromators. Typically, it can be tuned from the visible to the NIR region. For example, the TeO_2 noncollinear AOTF in our laboratory can be tuned from 600 to 1700 nm. Additionally, because the AOTF crystal is anisotropic, an incoming unpolarized light will be diffracted by the AOTF into two beams (ordinary and extraordinary) with orthogonal polarization. Simultaneous recording of images in the visible and NIR regions can, therefore, be accomplished by using one of the diffracted beams for the visible region and the other for the NIR region.

The main advantage of the InSb focal plane array (FPA) camera is its wide spectral range (from 1 to 5 μm). While this wide tuning range is attractive, it is seldom that the whole range is utilized in multispectral imaging instruments. This is because the tuning range of instruments is usually governed not by the camera but rather by the dispersive device (e.g., AOTF). As a consequence, InSb FPA is widely used in the middle IR region (from 3 to 5 μm) because it is the most sensitive detector in this region. Its use in the NIR region (from 1 to 2.5 μm) is not as widespread as in the middle-IR region because its sensitivity in this region is relatively lower than other NIR detectors. InGaAs detectors are known to have the highest sensitivity in the NIR region and can operate at room temperature. The latter feature not only makes these detectors easier to use but also reduces the size and cost

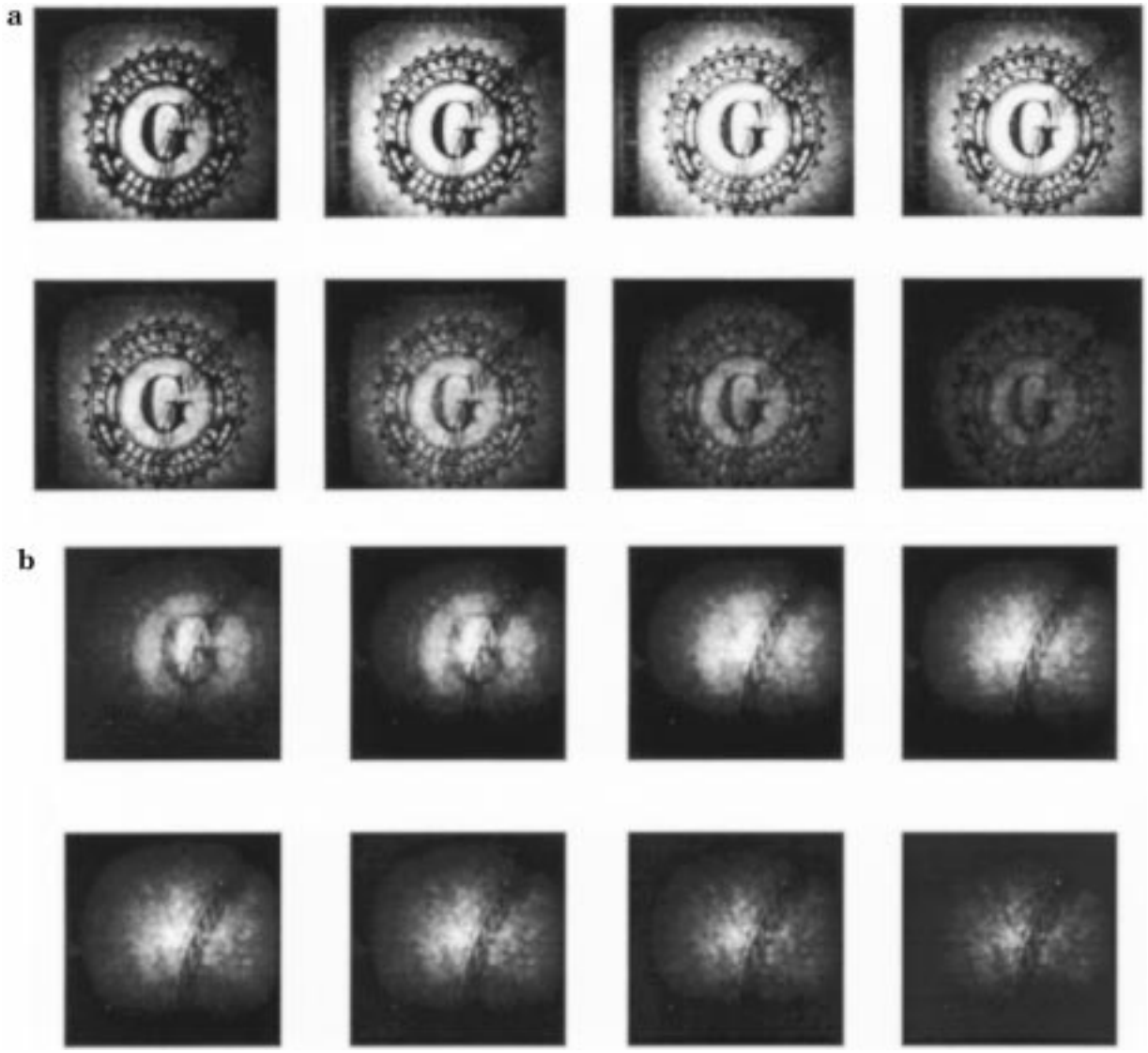

Figure 4. Images of the large letter G on the U.S. $5 bill taken (a) with the CCD camera at 650, 700, 750, 800, 850, 900, 950, and 1000 nm and (b) with the InGaAs camera at 1050, 1100, 1150, 1200, 1250, 1300, 1350, and 1400 nm.

of the instrument. As a consequence, InGaAs is usually the detector of choice for the NIR region. However, the FPA camera based in InGaAs was not available until recently. The 128 × 128 and the 320 × 240 InGaAs FPA cameras recently available from Sensors Unlimited Corp. make it possible, for the first time, to develop a sensitive multispectral imaging instrument for the NIR region at a fraction of the cost compared to those based on the InSb camera. The attractive features of this InGaAs camera, including its low cost (about 3 times lower than InSb) and high sensitivity, are as follows: Its room-temperature detectivity is 10^{13} jones, giving it a great advantage over InSb, HgCdTe, or PtSi sensors that require cooling. It is sensitive in the 900−1700-nm NIR band, and its quantum efficiency is better than 70% from below 1000 to beyond 1600 nm.

The information presented is provocative and clearly indicates that it is possible to use the AOTF, the InGaAs FPA camera, and the CCD camera to develop a low-cost, sensitive multispectral imaging instrument which is capable of simultaneous recording of spectral images in the visible and NIR region. The aim of this study is to develop such a low-cost, sensitive, and field-deployable instrument. In this instrument, an AOTF is used to provide two spectrally tunable diffracted beams. A CCD camera is used to detect one of the beams in the visible region. The other beam, detected by a FPA InGaAs camera, provides information in the NIR region. The instrumentation development and performance characteristics (imaging quality, resolution) of the instrument are reported in this paper. Preliminary results on the use of this instrument to characterize United States currency and to determine the chemical inhomogeneity of ethylene/vinyl acetate copolymers is also described.

EXPERIMENTAL SECTION

A schematic diagram of the multispectral imaging instrument is shown in Figure 1. As illustrated, light from a 250-W halogen tungsten lamp was collimated by a lens before passing through a noncollinear TeO_2 acoustooptic tunable filter (Matsushita Electronic Components Co., Ltd., model EFL F20R2). Two rf generators were used to drive the AOTF; namely, one with a frequency range of 96−53 MHz for the visible region (650−1050 nm) and the second for the near-IR region (1000−1650 nm) is with a

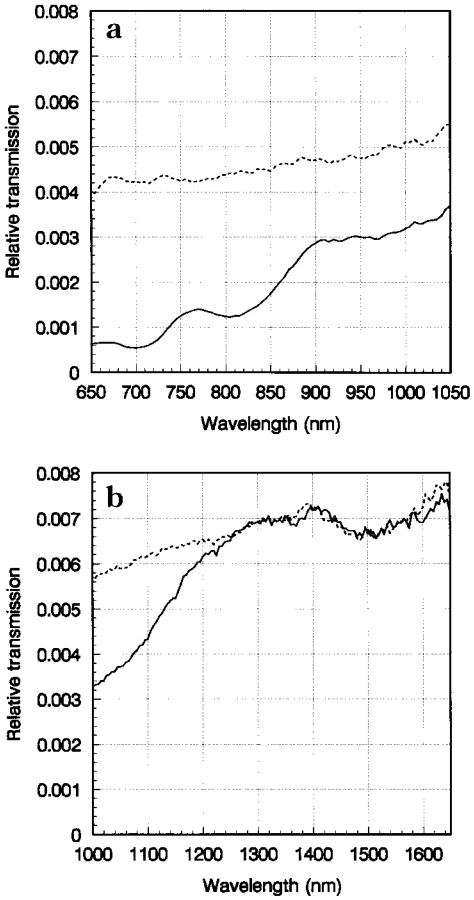

Figure 5. Transmission spectra of the letter G (solid line) and background (dotted line) on the U.S. $5 bill in the visible (a) and near-infrared regions (b), calculated from some of the images shown in Figure 4.

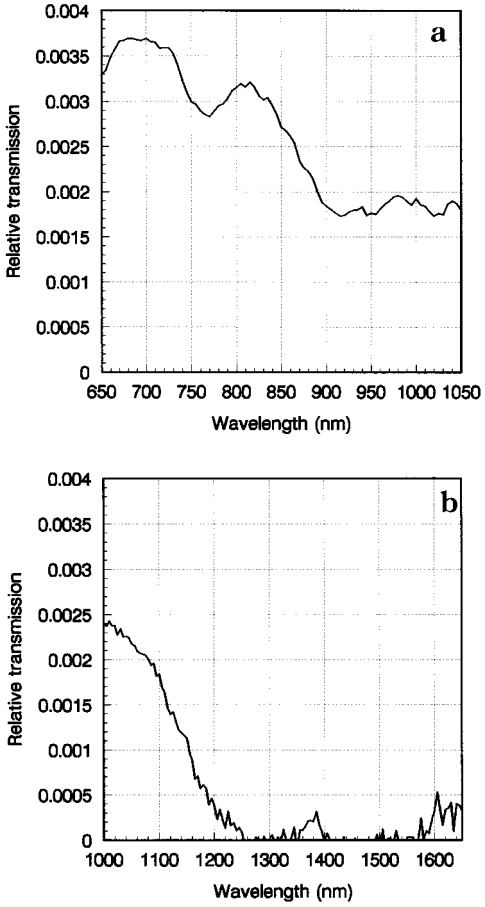

Figure 6. Differential spectra of the transmitted light through the letter G and background as shown in Figure 5.

frequency range of 59−35 MHz. The signals from these generators were amplified by a rf power amplifier (Minicircuits model MAV-11) before being connected to the AOTF. In addition to the transmitted beam, the AOTF diffracted unpolarized incident light into two diffracted beams that have orthogonal (horizontal and vertical) polarization. As illuminated, two diffracted beams not only have orthogonal polarization but also are spatially separated. One of the diffracted beams was used to record spectral imaging in the visible region while the other was for the near-infrared region. It is important to point out that because the AOTF crystal is anisotropic and the two diffracted beams have orthogonal polarization, the two beams will have slightly different wavelengths when a rf signal is applied to the AOTF. It is, therefore, important to separately calibrate the relationship between the applied rf frequency and the wavelength of the diffracted beam for each beam. The spectral images in the visible region were recorded by a thermoelectrically cooled silicon charge-coupled device (CCD) UV−visible camera (Spectral Source Instruments, model HPC-1) which has 512 × 512 pixels and is sensitive in the UV and visible regions (from 200 to 1100 nm). This silicon CCD camera does not detect any light at wavelengths longer than 1100 nm. An indium−gallium−arsenide (InGaAs) near-infrared FPA camera (Sensors Unlimited, model SU18-1.7RT/RS170), equipped with 128 × 128 pixels and sensitive in the 1000−1700 nm, was used to record images in the near-infrared (from 1000 to 1650 nm). The sensitivity of this InGaAs camera in the visible in negligible; i.e., no light at wavelengths shorter than 1000 nm is detected by this camera. Images in the visible were differentiated from those in the NIR by sequentially scanning the rf drivers and recording the images with the corresponding visible or NIR camera. Alternatively, the two rf drivers were synchronized with corresponding the two cameras to facilitate the simultaneous recording of the visible and NIR region. A digital frame grabber was used to transfer images from the cameras to a microcomputer for imaging processing.

Poly(ethylene-*co*-vinyl acetate) containing 9, 12, 18, and 25 wt % vinyl acetate was purchased from Aldrich Chemical. The copolymers came as beads and were pressed by a Carver Laboratory presser (model C) operated at 140 °C and 5000 lbs pressure into blocks of samples with a 2.54-cm diameter and 1 cm thick.

RESULTS AND DISCUSSION

I. Performance Characteristics of the Instrument. Performance of the system can be described in term of a modulation transfer function (MTF).[19,20] The MTF of an optical system is a measure of the contrast or the modulation (*M*) of the transmitted image relative to that of the object (i.e., the transfer, *T*) as a

(19) Bass, M. *Handbook of Optics*; McGraw-Hill: New York, 1995; Vol. 2, Chapter 32, pp 32.1−32.10.
(20) Williams, C. S.; Becklund, O. A. *Introduction to the Optical Transfer Function*; John Wiley: New York, 1989.

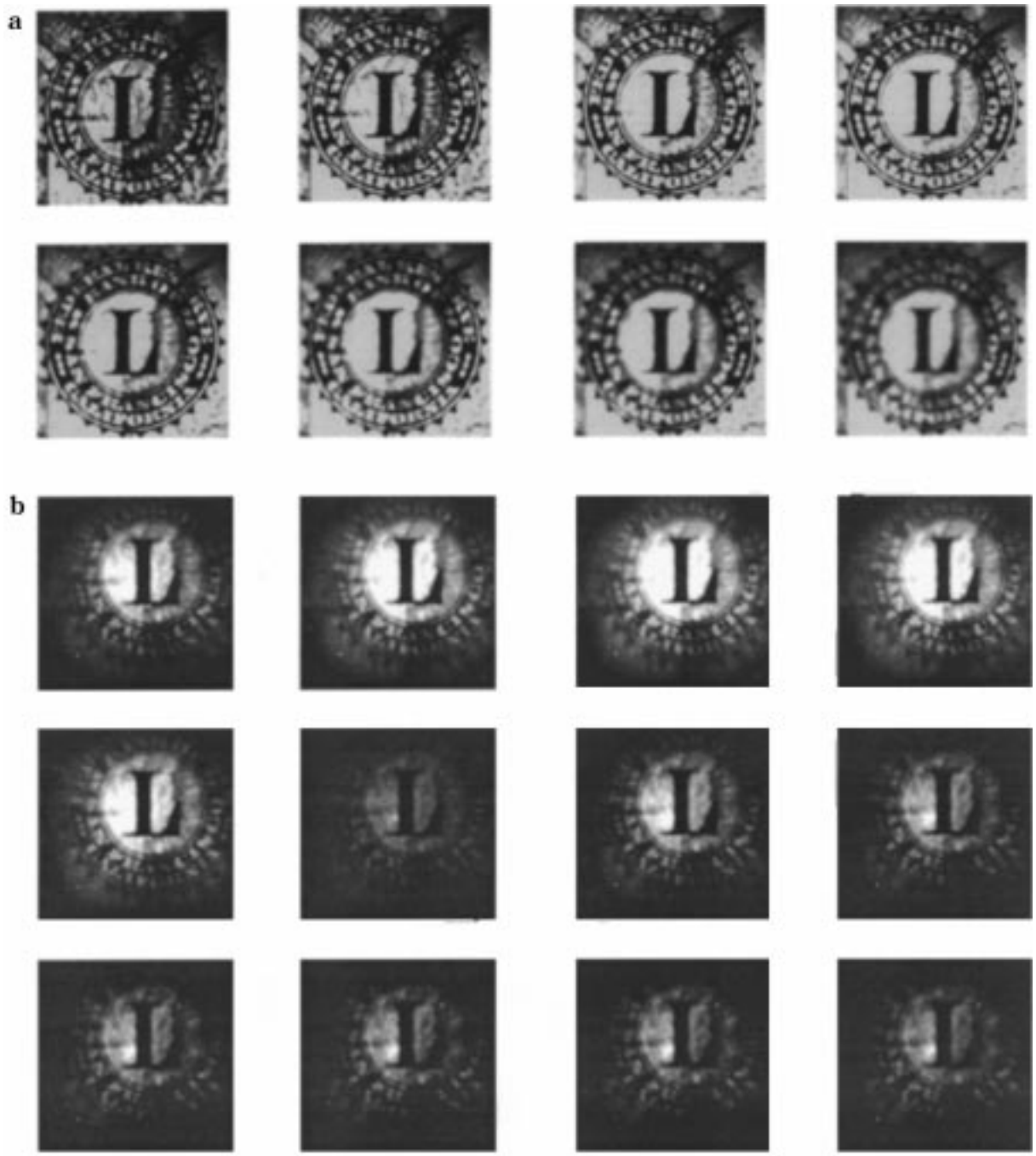

Figure 7. Images of the large letter L on the U.S. $1 bill taken (a) with the CCD camera at 650, 700, 750, 800, 850, 900, 950, and 1000 nm and (b) with the InGaAs camera at 1050, 1100, 1150, 1200, 1250, 1300, 1350, 1400, 1450, 1500, 1550, and 1600 nm.

function of the spatial frequency of the object.

$$M = \frac{E_{max} - E_{min}}{E_{max} + E_{min}}$$

$$T = M_{image}/M_{object}$$

$$\mathrm{MTF}\left(\frac{f}{f_{cutoff}}\right) = \frac{2}{\pi}\left[\cos^{-1}\left(\frac{f}{f_{cutoff}}\right) - \frac{f}{f_{cutoff}}\left[1 - \left(1 - \left(\frac{f}{f_{cutoff}}\right)^2\right]^{1/2}\right]\right]$$

where E_{max} and E_{min} are the maximum and minimum intensities, respectively, and f is the spatial frequency in line pairs per millimeter. f_{cutoff} is the cutoff frequency and is given by

$$f_{cutoff} = 1/\lambda \mathrm{FN}$$

where λ is the wavelength and FN is the F number of the optics.[19,20]

The USAF 1951 resolution target was used to determine the MTF of the AOTF-based system with the CCD at 650 nm and with the FPA camera at 1400 and 1600 nm. For comparison, the MTFs for the system in which the AOTF was replaced by interference filters at 650, 1400, and 1600 nm were also determined. The results obtained are shown in Figure 2. The MTFs obtained with the filters are similar to those obtained with the AOTF at the corresponding wavelengths. This suggests that any image perturbations induced by the AOTF are too insignificant

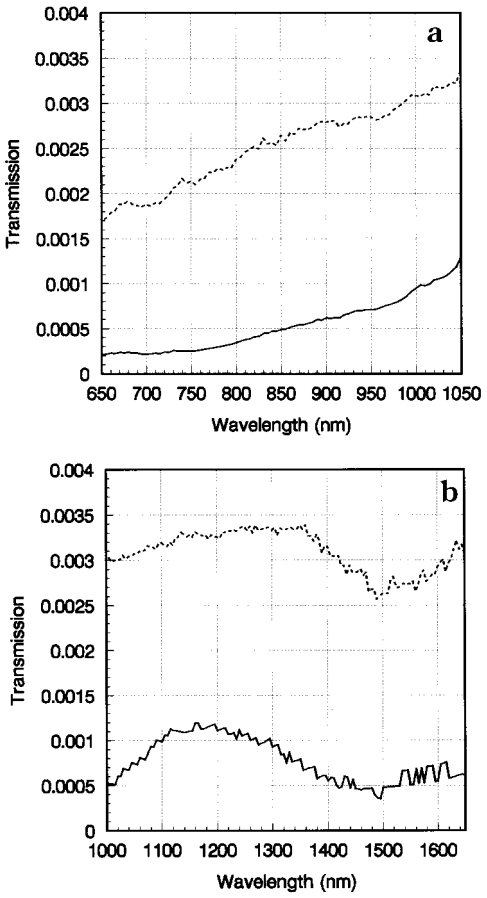

Figure 8. Transmission spectra of the letter L (solid line) and background (dotted line) on the U.S. $1 bill in the visible (a) and near-infrared regions (b), calculated from images, some of which are shown in Figure 7.

to be observed in the system. The image quality in the visible is much better than that in the near-infrared. This can be explained by the differences in resolution of two cameras; namely, the CCD camera used to record visible images has much better resolution than the near-infrared camera. Specifically, the visible CCD camera equipped with a SI-502A sensor (Scientific Imaging Technology, Inc.). This sensor has 512 × 512 pixels, and each pixel is 24 μm × 24 μm. This corresponds to 20 pair/mm in the horizontal and in the vertical. Conversely, the pixel size of the FPA near-infrared camera is 60 μm × 60 μm and there are 128 × 128 pixels in this camera. This corresponds to only about 8 pairs/mm and that may be the main reason for the lower imaging quality in the NIR. It is expected that better images can be obtained by replacing the present NIR camera with the high-resolution 12-bit InGaAs camera which has recently become commercially available. The pixel size in this camera is 40 μm × 40 μm and there are 320 × 240 pixels in the camera.

The spectral response of the instrument was determined by using the system to measure the absorption of ethanol. Shown in Figure 3a is the transmission of ethanol in 1-cm path length cell recording with the CCD camera. This spectrum is in good agreement with those obtained previously using a NIR spectrometer equipped with a single-element InGaAs detector.[7] It is important to note that this spectrum was recorded by a single pixel having dimension of 24 μm × 24 μm. Even more significant is the spectrum of ethanol in the near-infrared region recorded by the FPA InGaAs camera (Figure 3b). Again this spectrum was recorded by a single pixel of 60 μm × 60 μM, and the cell path length in this case was only 1 mm.

II. Applications. (1) Characterization of U.S. Currency. The imaging spectrometer was then used to measure spectra of U.S. currency. Images of the large letter G on the U.S. $5 bill were recorded, as the intensity of the transmitted light in two regions: visible (650−1050 nm at a 5-nm wavelength interval with the CCD camera) and the near-infrared (1000−1650 nm at a 5-nm interval with the InGaAs FPA camera). Figure 4a shows images recorded at 650, 700, 750, 800, 850, 900, 950, and 1000 nm) and Figure 4b are images at 1050, 1100, 1150, 1200, 1250, 1300, 1350, and 1400 nm (these are positive images in which white areas have higher transmission than dark areas). It is evident that the ink used to print the letter G absorbs light mainly in the visible region but becomes transparent in the near-infrared region beyond 1250 nm. This feature can be clearly seen when the spectra of one pixel in the background area and the spectra of one pixel on the symbol G are plotted (Figure 5). From these spectra, the difference between the spectrum of the sample (letter G) and of the background can be calculated. The results obtained, plotted in Figure 6, clearly show that there are large differences in the intensity of the light transmitted through the letter G in the visible region and nothing in the near-infrared region beyond 1250 nm. These results indicate that the ink in the large letter G has several

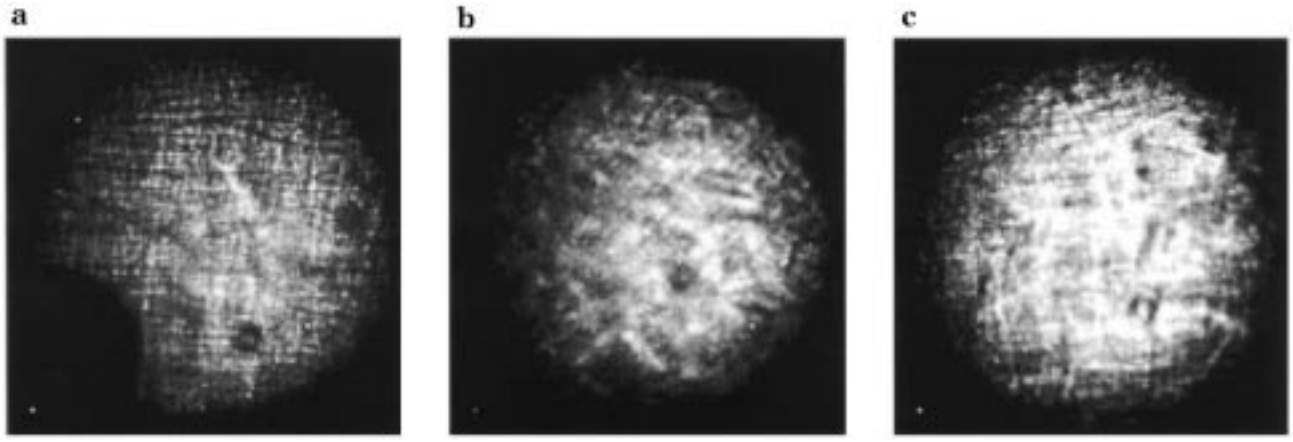

Figure 9. Images of ethylene/vinyl acetate copolymers with 9 (a), 12 (b), and 18 wt % (C) of vinyl acetate, taken at 1110 nm.

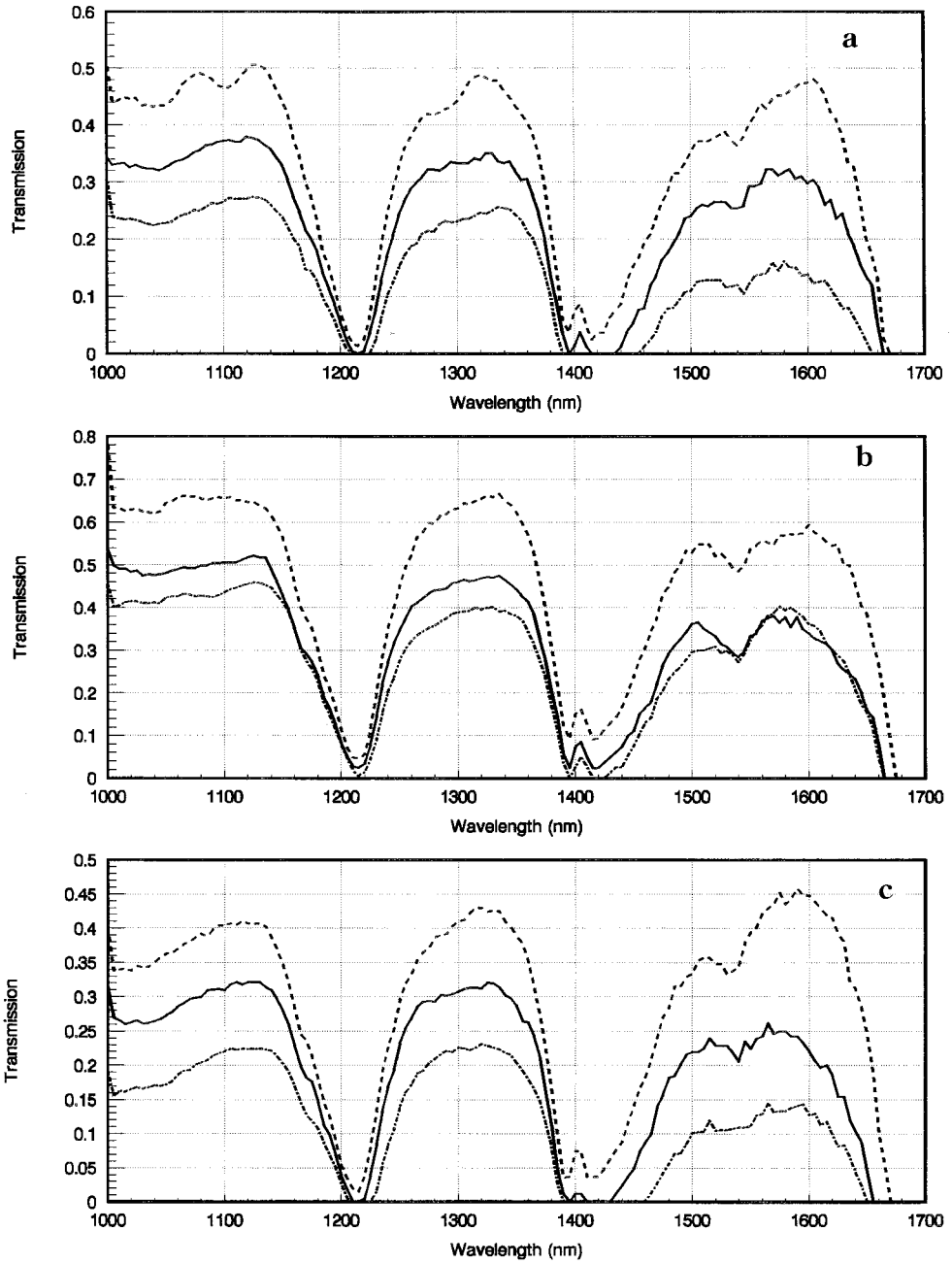

Figure 10. Transmission spectra of ethylene/vinyl acetate copolymers with 9 (a), 12 (b), and 18 wt % (c) of vinyl acetate, taken at three different positions corresponding to the bright (- - -), average (—) and dark (···) spots in images shown in Figure 9a–c, respectively.

absorption bands in the visible region (around 700, 820, and 1050 nm) and no absorption at all in the near-infrared region beyond 1250 nm. In fact, similar spectra were also found for the large letter G on the $10, the letter G on the $20, the large letter B on the old $50 as well as the large eagle symbol on the new $50 bill. Of particular interest is the images and spectra obtained for the large symbol L on the $1 as shown in Figures 7 and 8. Different from other bills, the letter L is clearly visualized throughout the visible and near-infrared regions. While it is difficult to properly quantify this observation with the current data, it is clear that the ink used to print this letter is different from the ink used in other bills.

(2) Chemical Inhomogeneities of Ethylene/Vinyl Acetate Copolymers. The near-infrared technique has been used extensively in recent years for qualitative and quantitative analysis of polymers. The technique can be used for the chemical analysis of individual polymers as well as for the determination of chemical compositions of copolymers. Care must be taken, however, to avoid possible errors when using the technique. The concerns are due to the nature of the polymers and the NIR measurements. Specifically, polymeric samples are known to be inhomogeneous because of a variety of factors including distribution of molecular weights in single-polymer samples and distribution of each polymer in the copolymer. Due to the chemical inhomogeneity, different NIR spectra can be obtained from the same sample if the spectra are measured with a NIR spectrometer, equipped with a single NIR detector, at different positions in a sample. The chemical information deduced from such spectra may be due not

only to the different in the chemical composition of the sample but also to the chemical inhomogeneity of the samples. Therefore, it is particularly important to determine the chemical homogeneity of a polymeric sample prior to applying the NIR technique to analyze its chemical composition. The present NIR multispectral imaging instrument is particularly suited for such task. Such considerations prompted us to use the NIR imaging spectrometer to investigate the chemical homogeneity of poly(ethylene/vinyl acetate) copolymers.

Images of poly(ethylene/vinyl acetate) copolymers containing 9, 12, and 18 wt% vinyl acetate, taken with the NIR imaging spectrometer at 1110 nm are shown in Figure 9a–c, respectively. As illustrated, all three samples exhibit a high degree of inhomogeneities. From images taken for each copolymers at different wavelengths (from 1000 to 1650 nm), the NIR spectra of different positions in each sample can be determined. Illustrated in Figure 10a are three NIR spectra corresponding to three different positions (dark, average and bright spot) on the 9% sample whose image is shown in Figure 9a. The bands at 1214, 1392, and 1418 nm can be assigned to the second overtones of the CH_2 stretching modes in ethylene and in vinyl acetate units.[21,22] The differences in the spectra shown in Figure 10a are due mainly to the differences in the relative concentration of the vinyl acetate unit in the sample; i.e., there are some regions where the concentration of the vinyl acetate unit in the copolymer is either lower or higher than 9%. Such inhomogeneity is not restricted to the 9% sample but is observed in other copolymers as well. Shown in Figure 10b and c are the spectra of 12% and 18% copolymers, respectively, calculated from the corresponding bright, average, and dark spots in Figure 9b and c. The contribution of scattering to the observed spectral differences is minimal because the differences are not of a continuous background with a slight and smooth decrease in the intensity (higher at shorter wavelength and lower at longer wavelength) as one would expect from scattering but rather have the same shape as the absorption spectrum of vinyl acetate. Furthermore, because the aperture of the collecting lens is rather large, any scattered light, if present, would be detected by the camera. The present multispectral image instrument has not been flat-field corrected. However, the observed spectral differences are not due to the flat-field distortion because such distortion, if present, would be the very similar for all samples.

Carefully inspection of spectra shown in Figure 10 reveals that two samples with different compositions can have essentially the same spectra. As an example, the spectrum that corresponds to the bright spot on the 9% sample is essentially the same as the spectrum of the average spot on 12% sample (Figure 11). This is hardly unexpected considering the high degree of inhomogeneity of these copolymers.

Taken together, the results presented clearly demonstrate that copolymers may exhibit a high degree of inhomogeneity. Because of the inhomogeneity, erroneous results may be obtained when the NIR technique is used to determine the chemical compositions of polymers and/or copolymers without any knowledge of the homogeneity of the samples. Especially, when a NIR spectrometer equipped with a single-element detector is used, it is important that the measurements are performed not at a single position on a single sample per concentration but rather on a set of samples per each concentration and on many different positions for each sample.

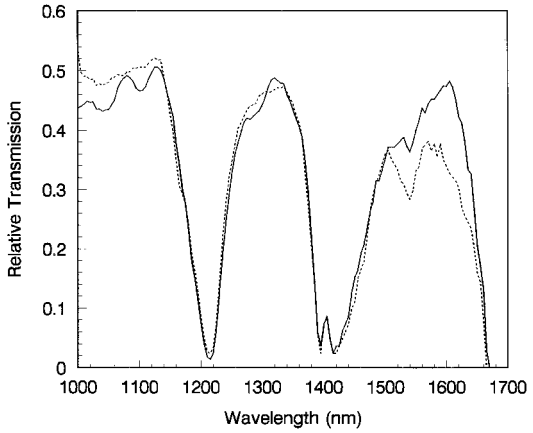

Figure 11. Transmission spectra calculated from the bright spot (—) in the image of 9% poly(ethylene-*co*-vinyl acetate) (Figure 9a) and the average spot (- - -) in the image of 12% poly(ethylene-*co*-vinyl acetate) (Figure 9b).

In summary, it has been demonstrated that the unique characteristics of the AOTF, namely, its ability to diffract an unpolarized incident beam into two diffracted beams with orthogonal polarization, have been exploited to develop the first multispectral image spectrometer which is capable of simultaneously measuring spectral images in the visible and NIR region. The imaging spectrometer is sensitive, inexpensive, and field deployable because it is based on the recently available InGaAs focal plane arrays camera which is low cost and can be sensitively operated at room temperature. Preliminary results indicate that the spectrometer can be used for measurements that, to date, are not possible. For example, visible and NIR absorption spectra of ink used to print U.S. currency and stock certificates can be readily measured directly from the samples. The results obtained will help to characterize samples as well as to ensure and to control quality during the production processes. More important are the results obtained on ethylene/vinyl acetate copolymers. The NIR spectral images clearly indicate that these copolymers exhibit a high degree of chemical inhomogeneity. Because of the possibility of inhomogeneity, it is very important that the homogeneity of polymers or copolymers be thoroughly understood before the NIR methods, especially those based on NIR spectrometers equipped with a single-element detector, are used for measurements. Finally, it is important to point out that inhomogeneities detected by the imaging spectrometer are dependent on its spatial resolution. Our efforts are, therefore, focused on increasing the spatial resolution of the spectrometer so that more detailed information on samples can be obtained.

ACKNOWLEDGMENT

The authors are grateful to Nader Dariavach, Marc Fischer, and Wencheng Liu for their competent assistance, and Prof. Charles Wilkie for use of his Carver Laboratory presser. Acknowledgment is made to the National Institutes of Health, National Center for Research Resources, and Biomedical Technology Program for financial support of this work.

Received for review June 12, 1998. Accepted September 2, 1998.

AC980647Q

(21) Shimoyama, N.; Hayano, S.; Matsukawa, K.; Inoue, H.; Ninomiya, T.; Ozaki, Y. *J. Polym. Sci. B* **1998**, *36*, 1529–1537.
(22) Khettry, A.; Hansen, M. G. *Polym. Eng. Sci.* **1996**, *36*, 1232–1237.